

Research Article

Effect of Li(I) and TiO₂ on the Upconversion Luminescence of Pr:Y₂SiO₅ and Its Photodegradation on Nitrobenzene Wastewater

Yi Yang,^{1,2} Guang-Zhi Xia,¹ Cheng Liu,¹ Jin-Hua Zhang,^{1,2} and Lian-Jun Wang^{1,2}

¹School of Environmental and Biological Engineering, Nanjing University of Science and Technology, Nanjing 210094, China

²Lianyungang Institute, Nanjing University of Science and Technology, Lianyungang 222006, China

Correspondence should be addressed to Yi Yang; yyi301@163.com

Received 16 April 2014; Accepted 27 August 2014

Academic Editor: Tian C. Zhang

Copyright © 2015 Yi Yang et al. This is an open access article distributed under the Creative Commons Attribution License, which permits unrestricted use, distribution, and reproduction in any medium, provided the original work is properly cited.

Based on the substrate of Pr:Y₂SiO₅ upconversion nanomaterials, lithium ion Li(I) doped Pr:Y₂SiO₅ and TiO₂ nanofilm coated Li,Pr:Y₂SiO₅ composites were prepared by using a sol-gel method. X-ray diffractometer, SEM, and fluorescence spectrometer have been employed to test the crystal structure, microimages, and upconversion luminescence performances. The doping of Li(I) affects highly the crystal transition of Pr:Y₂SiO₅ and X₂-Y₂SiO₅ phase was well formed by doping 8% Li(I). Furthermore, the doping of Li(I) also brings high luminance intensity of Pr:Y₂SiO₅ and contributes to a maximum intensity of 9.76×10^6 cps doped 8%. Too much of Li(I) doping would result in big crystal size and fluorescence quenching of Pr:Y₂SiO₅ material. However, the coating of TiO₂ nanofilm is not helping in increasing the upconversion fluorescence of Li,Pr:Y₂SiO₅ but is promoting the full use of the fluorescence. The luminescence intensities of TiO₂/Li,Pr:Y₂SiO₅ composites are getting down sharply with the coating amount since the luminescence emitted by Li,Pr:Y₂SiO₅ is quickly adsorbed in situ by the TiO₂ coating film. With the optimum coating concentration of 1%, the TiO₂/Li,Pr:Y₂SiO₅ composite shows excellent photodegradation performances on nitrobenzene wastewater, though it shows a low luminescence intensity. For 5 mg/L nitrobenzene wastewater, the composite presents a photodegradation rate of 97.08% in 4 hours.

1. Introduction

Currently, rare earth luminescent materials have been widely studied and used in information display, lighting, and other areas of optoelectronic devices supporting material [1–5], since its phosphor high luminous intensity and good shape can effectively improve the microscopic performance of the display. However, researches focused on the luminescence application in other fields, which the fluorescent materials emitted, are not as much as in the display fields. Some reports aimed at biological application, such as antibacterials [6, 7], and some researchers focus on environmental application of the luminescent materials [8, 9].

As one of the most researched luminescent material, yttrium silicates Y₂SiO₅ has a great potential application in many fields because of its high stability and good luminescence properties. Activated Y₂SiO₅ luminescent material

which is usually doped with other metal ions or activating agents is widely researched because of its much higher luminescence intensity than that of nonactivated material [10, 11]. Yttrium silicates Y₂SiO₅ has a particular geometry which leads to a possible replace of Y by other element ions, especially rare earth ions [12]. For example, Ce(III) doped Y₂SiO₅ can replace ZnS:Ag and can be used as blue phosphors for field emission display (FED); Tb(III) doped Y₂SiO₅ is a kind of cathode luminescence materials. Praseodymium ion Pr(III) has a similar ionic radius with Y ion but more suitable energy levels and longer excited state lifetimes than Y. As a result, higher energy photons and higher luminescence intensity could be emitted. Because of the small ionic radius, lithium ion Li(I) can easily get into the crystal lattice and replace the host atoms of Y₂SiO₅.

The photocatalytic behavior of TiO₂ has been studied extensively, because of the ability of nanoscale TiO₂ to

decompose a wide variety of inorganic and organic pollutants and toxic material in both liquid and gas phase systems [13–15], as well as the photocatalysis of nanoscale TiO_2 and its application for water purification [16, 17]. However, only ultraviolet light wavelength less than 387 nm, which is about 4% of the solar light, can be absorbed by pure anatase TiO_2 , since the energy gap of pure anatase TiO_2 is about 3.2 eV [18]. This became the main barrier which is limiting the wide use of TiO_2 as a photocatalyst. Many methods can be used to develop TiO_2 as a promising photocatalyst for wastewater treatment, such as surface modification [19, 20], doping with other metal ions, nonmetal ions and semiconductors [21–25], and oxygen vacancy generating [26].

The combination of anatase TiO_2 with upconversion materials could hopefully make more efficient use of solar energy in practical applications and provide a wide use of TiO_2 in photodegradation fields. In this study, Li(I) doped $\text{Pr:Y}_2\text{SiO}_5$ upconversion materials and anatase TiO_2 nanofilm coated $\text{Li,Pr:Y}_2\text{SiO}_5$ composite have been prepared and the luminescence intensities they emitted were tested. Nevertheless, the photodegradation performances of the as-prepared materials have been tested on the target pollutant of nitrobenzene wastewater.

2. Materials and Methods

2.1. Preparation of Samples. Praseodymium ion Pr(III), 1%, doped Y_2SiO_5 upconversion nanomaterials were prepared by following [8]. First, 0.1 mol/L praseodymium nitrate solution was added to the mixture (1:1, vol) of HNO_3 and H_2O dissolving 0.663 g Y_2O_3 . Heating was followed until the solution became a viscous mixture. A number of crystals were seed out after cooling down. The crystal was collected and dissolved in ethanol. Tetraethyl orthosilicate (TEOS) was added and mixed with the ethanol solution of the crystals. The obtained mixture was put into a water bath of 70°C until a gel was formed. The gel was dried in an oven at 104°C and then ground into powder. At last, the powder was calcined at a temperature of 950°C for 3 h in a muffle furnace to get the product $\text{Pr:Y}_2\text{SiO}_5$ upconversion nanomaterials.

Lithium ion Li(I) doped $\text{Pr:Y}_2\text{SiO}_5$ nanomaterials were prepared by adding 0.1 mol/L lithium nitrate to the praseodymium nitrate solution at the first step during the preparation of $\text{Pr:Y}_2\text{SiO}_5$. Then, sol-gel process and heat treatment parameters were followed as in the preparation of $\text{Pr:Y}_2\text{SiO}_5$ nanomaterials. The lithium ion doping concentrations, 2%, 6%, 8%, and 10%, were adjusted by changing the added volume of lithium nitrate solution. These products were called as $\text{Li,Pr:Y}_2\text{SiO}_5$.

The composite catalysts of $\text{TiO}_2/\text{Li,Pr:Y}_2\text{SiO}_5$ were prepared by adding the as-prepared $\text{Li,Pr:Y}_2\text{SiO}_5$ powder, which was ground and ultrasonic-dispersed in absolute alcohol for 30 min, to the mixture of titanium tetrabutoxide, absolute alcohol, and distilled water with a volume ratio of 1:7:2. The mixture was adjusted to pH 2.5 by using nitric acid. After stirring for 1 h, the suspension was put into a water bath at 70°C to form a white gel. Then, the gel was dried in an oven at 80°C and ground into powder. At last, the powder

was calcined at a temperature of 500°C for 2 h in a muffle furnace to get the product $\text{TiO}_2/\text{Li,Pr:Y}_2\text{SiO}_5$ composite catalyst. The TiO_2 concentrations, 0.3%, 0.5%, 1.0%, and 2.0%, were adjusted by changing the added volume of titanium tetrabutoxide.

2.2. Property Testing of Samples. A scanning electron microscopy (Hitachi S4800, SEM, Japan) was employed to characterize the microimages and particle size of the samples. X-ray diffractometer (D8 Advance, Bruker Corporation, German) was used to characterize the crystal form of the samples. The upconversion luminescence of the nanomaterials was tested by using a fluorescence spectrometer (FL3-TCSPC, Horiba Jobin Yvon Corporation, France). The exciting parameters were selected as 488 nm of the excitation wavelength, 370 nm of the optical filters, and 1 nm of the slit [27, 28].

Nitrobenzene wastewater, which was from a TNT factory and was diluted to 5 mg/L, was used as a target pollutant to test the photodegradation performances of the as-prepared upconversion nanomaterials. Triphosphor tube light, 100 W, was used as the exciting light source for the upconversion nanomaterials. The treatment time lasted for 1 h to 6 h. The degradation rate of nitrobenzene was calculated by comparing the ultraviolet absorption values at the wavelength of 267 nm to the original values of the nitrobenzene solution. The ultraviolet absorption values were tested by using an ultraviolet-visible spectrophotometer. The relationship of the nitrobenzene concentrations (x), in the range of 0.5–10 mg/L, with the ultraviolet absorption value (y), was determined by a linear equation $y = 9.06x - 0.312$, with a correlation R^2 of 0.99982.

3. Results and Discussion

3.1. $\text{Pr:Y}_2\text{SiO}_5$ with Different Li(I) Concentrations. Doping ions are known for changing crystal structure and crystal size, as well as light conversion performances for upconversion nanomaterials [8, 9]. Figure 1 shows the XRD patterns of $\text{Pr:Y}_2\text{SiO}_5$ with different Li(I) concentrations, 0%, 2%, 6%, 8%, and 10%.

It is known that Y_2SiO_5 has two types of crystal structure, low-temperature (X1) and high temperature (X2), when taking high temperature structure, with better emission performances. It is very interesting that the doping amount of Li(I) contributes a great effect to the crystal transition of Y_2SiO_5 materials. When the doping amounts of Li(I) are not bigger than 6%, the crystal form of samples belongs to low-temperature phase X1 molecular configuration ($\text{X1-Y}_2\text{SiO}_5$), which is corresponding to the PDF card number of #52-1810. However, when the doping amounts are high as 8%, the crystal forms of Y_2SiO_5 materials transfer from $\text{X1-Y}_2\text{SiO}_5$ to $\text{X2-Y}_2\text{SiO}_5$ phase, which is corresponding to the PDF card number of #21-1458, as shown in Figure 2. Generally, for $\text{X2-Y}_2\text{SiO}_5$ materials, heat treatment temperature up to 1350°C is needed [12], instead of 950°C in this study. It indicates that the doping of Li(I) can effectively decrease the crystallization temperature of Y_2SiO_5 and promotes the crystallization of $\text{X2-Y}_2\text{SiO}_5$ at a lower temperature. When the doping amount

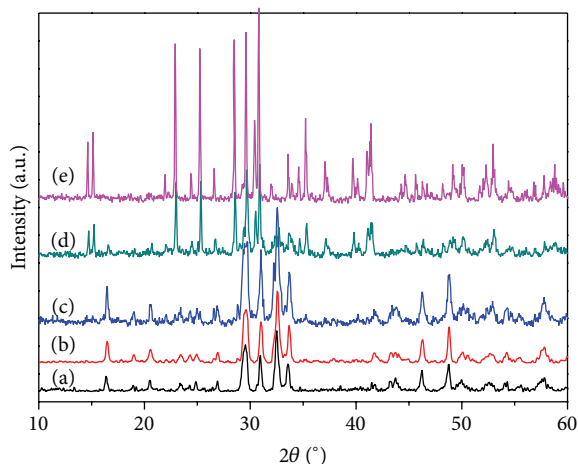


FIGURE 1: XRD patterns of Pr:Y₂SiO₅ doped different concentrations of Li(I). (a) 0%; (b) 2%; (c) 6%; (d) 8%; (e) 10%.

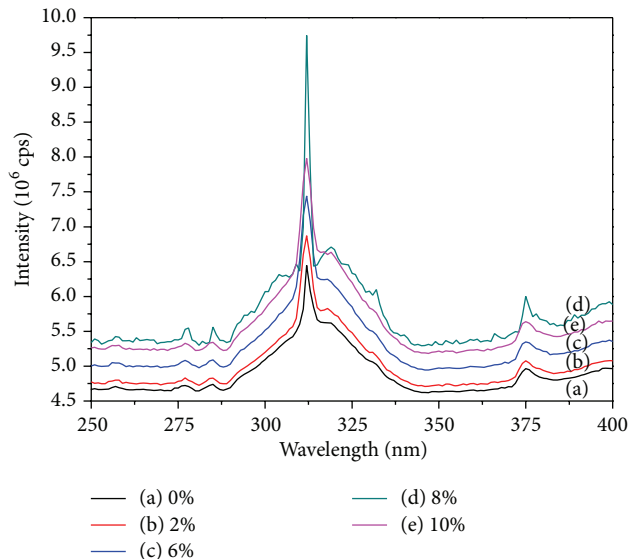
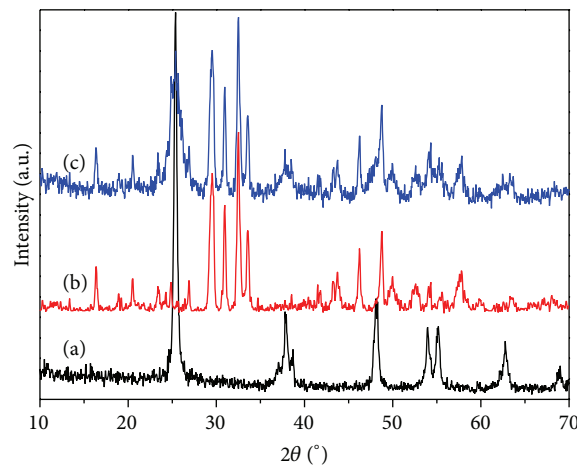


FIGURE 2: Emission spectra of Pr:Y₂SiO₅ doped different concentrations of Li(I). (a) 0%; (b) 2%; (c) 6%; (d) 8%; (e) 10%.

of Li(I) is increased to 10%, the diffraction peaks show much more sharp than that of 8%. The crystal sizes of Pr:Y₂SiO₅ with 8% and 10% Li(I) are 47.8 nm and 62.5 nm at 2θ angle 30.83°, respectively, which are calculated by the Scherrer equation [29]: $D = K\lambda/(\beta \cos \theta)$, where D is the crystal size (nm); K is 0.89, the Scherrer constant; θ is the diffraction angle at which the diffraction peaks are located (°); β is the full width at half maximum (FWHM) of the main diffraction peaks (rad), which is located at the 2θ angle of 30.83° in this situation; λ is 0.154056 nm, the X-ray wavelength.

Figure 2 shows the upconversion luminescence emission spectra of Pr:Y₂SiO₅ doped with different concentrations of Li(I). Since the excitation wavelength is set on 488 nm, the peaks of the upconversion luminescence emission spectra are located at 312 nm, instead of 425 nm and 360 nm of



(a) TiO₂ (anatase)
(b) Li,Pr:Y₂SiO₅
(c) TiO₂/Li,Pr:Y₂SiO₅

FIGURE 3: XRD patterns of samples. (a) Commercial anatase TiO₂; (b) Li,Pr:Y₂SiO₅; (c) TiO₂/Li,Pr:Y₂SiO₅.

the excitation wavelength and the emission spectra peaks, respectively [8].

As the Li(I) doping amount increases, the intensity of the emission spectra is increasing gradually but is getting down at the doping amount of 10%, as shown in Figure 2. Sample doped with 8% Li(I) shows the strongest luminescence intensity of 9.76×10^6 cps (count per second), which is about 1.5 times of the blank sample Pr:Y₂SiO₅ (0% Li) emitted at the wavelength of 312 nm. Compared to lower doping samples, sample doped with 8% Li(I) emits much stronger upconversion luminescence, which has more intact X2-Pr:Y₂SiO₅ structures according to the test results in Figure 1. On the other hand, too much of Li(I) doping amount, as shown in Figure 1, would result in big crystal size of Pr:Y₂SiO₅ nanomaterials. For upconversion luminescence nanomaterials, a smaller crystal size hopefully contributes to higher upconversion efficiency. However, it is believed that too high doping concentration of exotic ions would result in luminescent quenching [30]. As a result, the doping concentration of 10% Li(I) results in a low luminescence intensity, as shown in Figure 2. Therefore, Pr:Y₂SiO₅ upconversion nanomaterial doping 8% Li(I), which has a smaller crystal size and less fluorescence quenching, emits much stronger luminescence than that of doping 10% Li(I), as shown in Figure 2.

3.2. Testing of TiO₂/Li,Pr:Y₂SiO₅ Composites. It is different with doping of ions; doping of nanomaterials would seldom change the crystal structure of the host material. Figure 3 shows the XRD patterns of three kinds of samples, commercial nanometer TiO₂ (anatase), as-prepared Li,Pr:Y₂SiO₅ (8% Li), and as-prepared TiO₂/Li,Pr:Y₂SiO₅ (1% TiO₂).

As shown in Figure 3, the XRD pattern of sample (c) is seemingly the combination of that of sample (a) and sample (b), which clearly corresponds to the XRD diffraction peaks

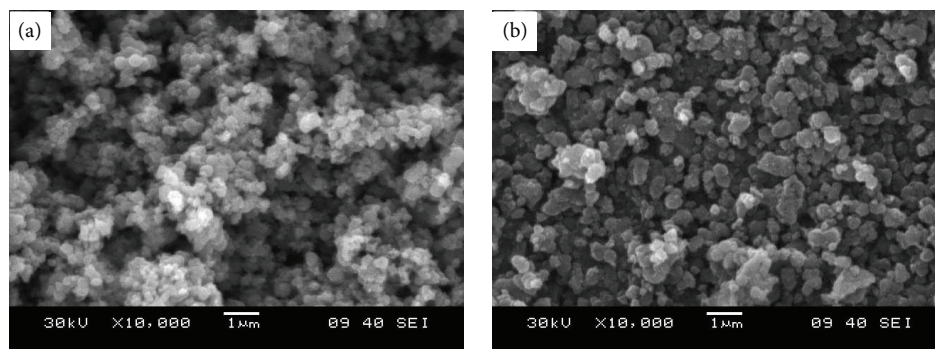


FIGURE 4: SEM photos of (a) $\text{Li,Pr:Y}_2\text{SiO}_5$ and (b) $\text{TiO}_2/\text{Li,Pr:Y}_2\text{SiO}_5$ nanomaterials.

of TiO_2 and $\text{Li,Pr:Y}_2\text{SiO}_5$. However, comparing the intensities of diffraction peaks belonging to TiO_2 , the diffraction intensities of sample (c) are much lower than those of sample (a), commercial anatase TiO_2 . On the other hand, the diffraction intensities belonging to $\text{Li,Pr:Y}_2\text{SiO}_5$ do not show big differences between $\text{Li,Pr:Y}_2\text{SiO}_5$ and its composite. It indicates that TiO_2 and $\text{Li,Pr:Y}_2\text{SiO}_5$ are two independent materials coexisted in the composite of $\text{TiO}_2/\text{Li,Pr:Y}_2\text{SiO}_5$. Titanium dioxide probably in the form of films exists on the surface of $\text{Li,Pr:Y}_2\text{SiO}_5$ particles, which also can be suggested by the SEM photos of the samples, as shown in Figure 4.

Figure 4(a) shows SEM photo of $\text{Li,Pr:Y}_2\text{SiO}_5$ particles, which presents regular but partially reunited spherical particles in the diameter of 300 nm to 500 nm. A little different from $\text{Li,Pr:Y}_2\text{SiO}_5$ sample, $\text{TiO}_2/\text{Li,Pr:Y}_2\text{SiO}_5$ nanoparticles show good dispersibility and are a little big in size, which is in the range of 500 nm to 800 nm, as shown in Figure 4(b). Much bigger particle sizes in SEM than those of XRD indicate that every single particle is composed of several crystals which makes it difficult to disperse the $\text{Li,Pr:Y}_2\text{SiO}_5$ powders fully in the preparation process. Energy dispersive X-ray spectrometer (EDS) testing on the sample surface of Figure 4(b) shows that Ti and O are the majority of elements, while Si and Y are the minority of elements. It is difficult to find element information of Li and Pr in the EDS testing. It suggests that TiO_2 film gives intact coating for $\text{Li,Pr:Y}_2\text{SiO}_5$ particles in a thickness of about 100 nm to 150 nm.

Figure 5 shows the upconversion emission spectra of $\text{Li,Pr:Y}_2\text{SiO}_5$ with different concentrations of TiO_2 . It is very different to the situation of doping with Li(I) and Pr(III); the upconversion luminescence intensities are decreasing with the coating amount of TiO_2 , instead of increasing by the doping amount of Li(I) and Pr(III). This should be attributed to the semiconductor characteristics of TiO_2 . It is known that titanium dioxide is a kind of *n*-type semiconductor material with a band gap of 3.2 eV (for anatase). When it is exposed to ultraviolet light whose wavelength is less than 387.5 nm, energy would be added to valence electron and it would be excited by photon and would leap from the valence band (VB) to the conduction band (CB), where it can move freely around the crystal in the form of photoelectron [31]. As a result, a hole is left behind in the valence band. On the occasion

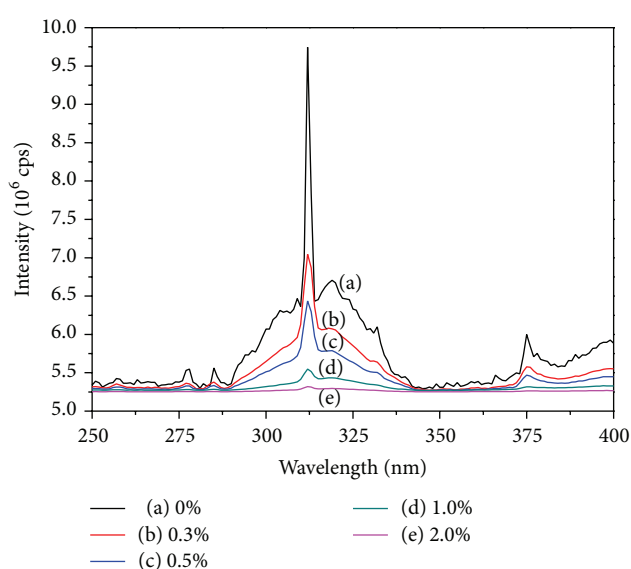


FIGURE 5: Emission spectra of $\text{Li,Pr:Y}_2\text{SiO}_5$ with different concentrations of TiO_2 . (a) 0%; (b) 0.3%; (c) 0.5%; (d) 1.0%; (e) 2.0%.

of nanoscale TiO_2 coating on the upconversion material $\text{Li,Pr:Y}_2\text{SiO}_5$, the luminescence emitted by $\text{Li,Pr:Y}_2\text{SiO}_5$ is absorbed in situ by the TiO_2 coating film. When more of TiO_2 film is coated, less of the luminescence intensity can be tested. When the coating amount of TiO_2 film is up to 1%, the intensity of the emission spectra is very low. There almost can not be found luminescence peaks on the emission spectra of the sample with 2% of TiO_2 , as shown in Figure 5. It means that too much of coating TiO_2 would absorb out all the luminescence that the upconversion material $\text{Li,Pr:Y}_2\text{SiO}_5$ emitted. Therefore, the coating amount of 1% could be a balance point or optimum value for the composite of $\text{TiO}_2/\text{Li,Pr:Y}_2\text{SiO}_5$ nanomaterials.

3.3. Photodegradation of Nitrobenzene Wastewater. Nitrobenzene wastewater, which is an environmental priority control pollutant, usually comes from the factories manufacturing medicines, pesticides, plastics, and explosives. The

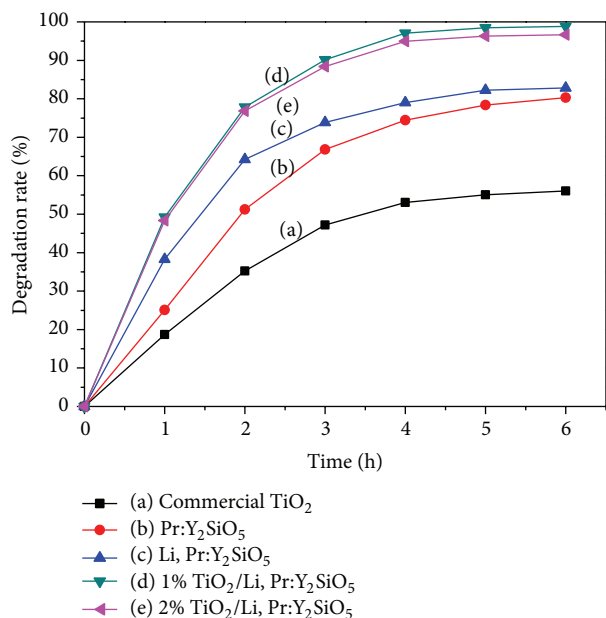


FIGURE 6: The photodegradation performances of nanomaterial samples. (a) Commercial TiO₂; (b) Pr:Y₂SiO₅; (c) Li,Pr:Y₂SiO₅; (d) 1% TiO₂/Li,Pr:Y₂SiO₅; (e) 2% TiO₂/Li,Pr:Y₂SiO₅.

degradation-resistant pollutant, which is attributed to its particular molecular structures, is difficult to degrade by normal methods [32]. In this study, 5 mg/L nitrobenzene wastewater and 1.5 g/L photocatalysts are used to test the photodegradation performances of as-prepared samples. The photodegradation curves of nitrobenzene wastewater with the photocatalysts of commercial nanometer anatase TiO₂, Pr:Y₂SiO₅, Li,Pr:Y₂SiO₅, 1% TiO₂/Li,Pr:Y₂SiO₅ (with 1% of TiO₂, similarly hereinafter), and 2% TiO₂/Li,Pr:Y₂SiO₅, are shown in Figure 6. All the data in Figure 6 are the mean values measured 3 times.

Samples TiO₂/Li,Pr:Y₂SiO₅, curves (d) and (e), show excellent photodegradation performances, but commercial TiO₂ shows the worst in the samples. Nanoscale TiO₂ is known for its good photocatalysis performances on pollutions under ultraviolet light. However, very different situation for nanoscale TiO₂ would arise when it is exposed to visible light. Thus, in this study, compounding of TiO₂ with Li,Pr:Y₂SiO₅ nanomaterials, which can upconvert visible light to ultraviolet light, would significantly improve the photocatalysis performances of TiO₂ under visible light, as shown in Figure 6. Although the luminescence intensities of TiO₂/Li,Pr:Y₂SiO₅ composite are far lower than that of Li,Pr:Y₂SiO₅ nanomaterials, as shown in Figure 5, it does not mean that the upconversion processes of Li,Pr:Y₂SiO₅ in the composite are stopped. It is still working well in the form of promoting and strengthening the photocatalysis of TiO₂ by providing high energy photons, instead of in the form of high intensity of upconversion luminescence emit out of the materials which can be tested, as shown in Figures 5 and 6. On the other hand, too much coating of TiO₂ film would not only

increase the barrier of visible light to Li,Pr:Y₂SiO₅ nanomaterials, which weakens the intensity of incident light, but also decrease the proportion of Li,Pr:Y₂SiO₅ in the composite, in which the conversion of visible light to ultraviolet light is provided. Therefore, TiO₂/Li,Pr:Y₂SiO₅ coating with 2% TiO₂ shows a little bit poor photodegradation performance than that with 1% TiO₂, as shown in Figure 6.

For samples Pr:Y₂SiO₅ and Li,Pr:Y₂SiO₅, their photodegradation performances show high consistency with the intensities of upconversion luminescence which they emitted; the former is lower than the latter. Because of lack of direct or quick conversion ultraviolet light, high energy photons, to hydroxyl radical (\bullet OH) [33], which is one of the most strong oxidizability matter, two of the upconversion nanomaterials show much more poor photodegradation performances than TiO₂/Li,Pr:Y₂SiO₅ composites.

4. Conclusions

Lithium ion Li(I) doped Pr:Y₂SiO₅ and TiO₂ nanofilm coated Li,Pr:Y₂SiO₅ composites were prepared by using a sol-gel method. The doping amount of Li(I) plays an important role on the upconversion luminescence of the nanomaterial which reaches a maximum intensity of 9.76×10^6 cps with the doping concentration of 8%. The coating of TiO₂ nanofilm leads the luminescence intensity of TiO₂/Li,Pr:Y₂SiO₅ composite to get down sharply, since the luminescence emitted by Li,Pr:Y₂SiO₅ is adsorbed in situ by the TiO₂ coating film. As a result, the TiO₂/Li,Pr:Y₂SiO₅ composite with 1% TiO₂, which presents a low luminescence intensity, shows the excellent photodegradation performance on nitrobenzene wastewater. For 5 mg/L of nitrobenzene wastewater, the photodegradation rate is up to 97.08% and 98.82% in 4 h and 6 h, respectively.

Conflict of Interests

The authors declare that there is no conflict of interests regarding the publication of this paper.

Acknowledgment

The work was supported by the Foundation of Jiangsu Environmental Protection Department, China (no. 2012015).

References

- [1] S. Marks, J. G. Heck, M. H. Habicht, P. Oña-Burgos, C. Feldmann, and P. W. Roesky, "[Ln(BH₄)₂(THF)₂](Ln = Eu, Yb)—a highly luminescent material. Synthesis, properties, reactivity, and NMR studies," *Journal of the American Chemical Society*, vol. 134, no. 41, pp. 16983–16986, 2012.
- [2] L. Zhang, B. Liu, and S. Dong, "Bifunctional nanostructure of magnetic core luminescent shell and its application as solid-state electrochemiluminescence sensor material," *Journal of Physical Chemistry B*, vol. 111, no. 35, pp. 10448–10452, 2007.
- [3] V. Martínez-Martínez, R. García, L. Gómez-Hortigüela, R. S. Llano, J. Pérez-Pariente, and I. López-Arbeloa, "Highly

- luminescent and optically switchable hybrid material by one-pot encapsulation of dyes into MgAPO-11 unidirectional nanopores,” *ACS Photonics*, vol. 1, no. 3, pp. 205–211, 2014.
- [4] V. B. Taxak and S. P. Khatkar, “Synthesis, characterization and luminescent properties of Eu/Tb-doped LaSrAl₃O₇ nanophosphors,” *Journal of Alloys and Compounds*, vol. 549, pp. 135–140, 2013.
- [5] D. Giaume, V. Buissette, K. Lahlil et al., “Emission properties and applications of nanostructured luminescent oxide nanoparticles,” *Progress in Solid State Chemistry*, vol. 33, no. 2-4, pp. 99–106, 2005.
- [6] W. Wang, Q. Shang, W. Zheng et al., “A novel near-infrared antibacterial material depending on the upconverting property of Er³⁺-Yb³⁺-Fe³⁺ tridoped TiO₂ nanopowder,” *Journal of Physical Chemistry C*, vol. 114, no. 32, pp. 13663–13669, 2010.
- [7] M. Wang, G. Abbineni, A. Clevenger, C. Mao, and S. Xu, “Upconversion nanoparticles: Synthesis, surface modification and biological applications,” *Nanomedicine: Nanotechnology, Biology, and Medicine*, vol. 7, no. 6, pp. 710–729, 2011.
- [8] Y. Yang, C. Liu, P. Mao, and L.-J. Wang, “Upconversion luminescence and photodegradation performances of Pr doped Y₂SiO₅ nanomaterials,” *Journal of Nanomaterials*, vol. 2013, Article ID 427370, 7 pages, 2013.
- [9] G. Feng, S. Liu, Z. Xiu et al., “Visible light photocatalytic activities of TiO₂ nanocrystals doped with upconversion luminescence agent,” *Journal of Physical Chemistry C*, vol. 112, no. 35, pp. 13692–13699, 2008.
- [10] T. Anh, P. Benalloul, C. Barthou, L. T. Giang, N. Vu, and L. Minh, “Luminescence, energy transfer, and upconversion mechanisms of Y₂O₃ nanomaterials doped with Eu³⁺, Tb³⁺, Tm³⁺, Er³⁺, and Yb³⁺ ions,” *Journal of Nanomaterials*, vol. 2007, Article ID 48247, 10 pages, 2007.
- [11] N. Nguyen, M. H. Nam, T. K. Anh, L. Q. Minh, and E. Tanguy, “Optical properties of Eu³⁺ doped Y₂O₃ nanophosphors,” *Advances in Natural Sciences*, vol. 6, pp. 119–123, 2006.
- [12] J. Lin, Q. Su, S. Wang, and H. Zhang, “Influence of crystal structure on the luminescence properties of bismuth (III), europium(III) and dysprosium(III) in Y₂SiO₅,” *Journal of Materials Chemistry*, vol. 6, no. 2, pp. 265–269, 1996.
- [13] M. R. Hoffmann, S. T. Martin, W. Choi, and D. W. Bahnemann, “Environmental applications of semiconductor photocatalysis,” *Chemical Reviews*, vol. 95, no. 1, pp. 69–96, 1995.
- [14] K. Palmisano, V. Augugliaro, A. Sclafani, and M. Schiavello, “Activity of chromium-ion-doped titania for the dinitrogen photoreduction to ammonia and for the phenol photodegradation,” *Journal of physical chemistry*, vol. 92, no. 23, pp. 6710–6713, 1988.
- [15] B. Neumann, P. Bogdanoff, H. Tributsch, S. Sakthivel, and H. Kisch, “Electrochemical mass spectroscopic and surface photovoltage studies of catalytic water photooxidation by undoped and carbon-doped titania,” *Journal of Physical Chemistry B*, vol. 109, no. 35, pp. 16579–16586, 2005.
- [16] T. Ochiai and A. Fujishima, “Photoelectrochemical properties of TiO₂ photocatalyst and its applications for environmental purification,” *Journal of Photochemistry and Photobiology C: Photochemistry Reviews*, vol. 13, no. 4, pp. 247–262, 2012.
- [17] T. Ochiai, K. Masuko, S. Tago et al., “Synergistic water-treatment reactors using a TiO₂-modified Ti-mesh filter,” *Water*, vol. 5, no. 3, pp. 1101–1115, 2013.
- [18] J. M. Mwabora, T. Lindgren, E. Avendaño et al., “Structure, composition, and morphology of photoelectrochemically active TiO_{2-x}N_x thin films deposited by reactive DC magnetron sputtering,” *Journal of Physical Chemistry B*, vol. 108, no. 52, pp. 20193–20198, 2004.
- [19] L. Liu, C. Zhao, and F. Yang, “TiO₂ and polyvinyl alcohol (PVA) coated polyester filter in bioreactor for wastewater treatment,” *Water Research*, vol. 46, no. 6, pp. 1969–1978, 2012.
- [20] S. Yang, J.-S. Gu, H.-Y. Yu et al., “Polypropylene membrane surface modification by RAFT grafting polymerization and TiO₂ photocatalysts immobilization for phenol decomposition in a photocatalytic membrane reactor,” *Separation and Purification Technology*, vol. 83, no. 1, pp. 157–165, 2011.
- [21] M. Farbod and M. Kajbafvala, “Effect of nanoparticle surface modification on the adsorption-enhanced photocatalysis of Gd/TiO₂ nanocomposite,” *Powder Technology*, vol. 239, pp. 434–440, 2013.
- [22] J. L. Rodríguez, T. Poznyak, M. A. Valenzuela, H. Tiznado, and I. Chairez, “Surface interactions and mechanistic studies of 2,4-dichlorophenoxyacetic acid degradation by catalytic ozonation in presence of Ni/TiO₂,” *Chemical Engineering Journal*, vol. 222, pp. 426–434, 2013.
- [23] W. Zhang, L. Zou, and L. Wang, “A novel charge-driven self-assembly method to prepare visible-light sensitive TiO₂/activated carbon composites for dissolved organic compound removal,” *Chemical Engineering Journal*, vol. 168, no. 1, pp. 485–492, 2011.
- [24] N. Liu, X. Chen, J. Zhang, and J. W. Schwank, “A review on TiO₂-based nanotubes synthesized via hydrothermal method: formation mechanism, structure modification, and photocatalytic applications,” *Catalysis Today*, vol. 225, pp. 34–51, 2014.
- [25] Q. Wang, X. Wang, X. Li, Y. Cai, and Q. Wei, “Surface modification of PMMA/O-MMT composite microfibers by TiO₂ coating,” *Applied Surface Science*, vol. 258, no. 1, pp. 98–102, 2011.
- [26] D. L. Hou, H. J. Meng, L. Y. Jia, X. J. Ye, H. J. Zhou, and X. L. Li, “Oxygen vacancy enhanced the room temperature ferromagnetism in Ni-doped TiO₂ thin films,” *Physics Letters A*, vol. 364, no. 3-4, pp. 318–322, 2007.
- [27] C. Hu, C. Sun, J. Li, Z. Li, H. Zhang, and Z. Jiang, “Visible-to-ultraviolet upconversion in Pr³⁺:Y₂SiO₅ crystals,” *Chemical Physics*, vol. 325, no. 2-3, pp. 563–566, 2006.
- [28] C. L. Sun, J. F. Li, C. H. Hu, H. M. Jiang, and Z. K. Jiang, “Ultraviolet upconversion in Pr³⁺:Y₂SiO₅ crystal by Ar⁺ laser (488 nm) excitation,” *European Physical Journal D*, vol. 39, no. 2, pp. 303–306, 2006.
- [29] G. Ramakrishna, H. Nagabhushana, D. V. Sunitha, S. C. Prashantha, S. C. Sharma, and B. M. Nagabhushana, “Effect of different fuels on structural, photo and thermo luminescence properties of solution combustion prepared Y₂SiO₅ nanopowders,” *Spectrochimica Acta A: Molecular and Biomolecular Spectroscopy*, vol. 127, pp. 177–184, 2014.
- [30] L. Jia, Z. Shao, Q. Lü, Y. Tian, and J. Han, “Optimum europium doped aluminoborates phosphors and their photoluminescence properties under VUV and UV excitation,” *Optics and Laser Technology*, vol. 54, pp. 79–83, 2013.
- [31] K. Nakata, T. Ochiai, T. Murakami, and A. Fujishima, “Photoenergy conversion with TiO₂ photocatalysis: new materials and recent applications,” *Electrochimica Acta*, vol. 84, pp. 103–111, 2012.

- [32] X. Fu, J. Ji, W. Tang, W. Liu, and S. Chen, "Mo-W based copper oxides: Preparation, characterizations, and photocatalytic reduction of nitrobenzene," *Materials Chemistry and Physics*, vol. 141, no. 2-3, pp. 719–726, 2013.
- [33] S. A. V. Eremia, D. Chevalier-Lucia, G.-L. Radu, and J.-L. Marty, "Optimization of hydroxyl radical formation using TiO_2 as photocatalyst by response surface methodology," *Talanta*, vol. 77, no. 2, pp. 858–862, 2008.



Hindawi

Submit your manuscripts at
<http://www.hindawi.com>

